ECCOMAS Congress 2016
VII European Congress on Computational Methods in Applied Sciences and Engineering
M. Papadrakakis, V. Papadopoulos, G. Stefanou, V. Plevris (eds.)
Crete Island, Greece, 5–10 June 2016

MESH GENERATION FOR THE 2D NURBS-ENHANCED FINITE ELEMENT METHOD

Ruben Sevilla, Luke Rees and Oubay Hassan

Zienkiewicz Centre for Computational Engineering
College of Engineering, Swansea University, Swansea, SA1 8EN, Wales, UK.
e-mail: R.Sevilla@swansea.ac.uk

Keywords: triangular mesh, NEFEM, geometric features, high-order finite elements, NURBS.

Abstract. *The first method that enables the fully automatic generation of triangular meshes suitable for the so-called NURBS-enhanced finite element method (NEFEM) is presented. The methodology is able to produce meshes of the desired element size irrespectively of the geometric complexity and always encompassing the exact boundary representation of the domain given by NURBS curves. The strategy enables to completely circumvent the time consuming process of de-featuring complex geometric models before a finite element mesh suitable for the analysis can be produced. Numerical examples demonstrate the applicability of the proposed approach and the advantages compared to traditional finite element mesh generators.*

1 INTRODUCTION

The last decade has seen an increasing interest in high-order accurate methods due to their ability to reduce the dissipation and/or dispersion associated to traditional low-order methods. This is particularly attractive in computational electromagnetics [1, 2, 3] and computational fluid dynamics [4, 5, 6, 7] due to the need to propagate waves or vortices over long distances.

The need of curved elements to fully exploit the benefits of high-order methods has prompted a great interest in the research community on the generation of high-order curvilinear meshes [8, 9, 10, 11, 12, 13]. In terms of computational efficiency, very coarse curvilinear meshes and very high-order approximations are preferred, but the effect of geometric inaccuracies becomes evident. In [14] it was showed that the error induced by the isoparametric formulation can be up to one order of magnitude higher than a formulation with an exact boundary representation. In addition, complex geometries of large scale objects often contain very small geometric features, making necessary to produce extremely refined meshes in some regions. In many occasions, it is necessary to invest a non-negligible amount of time removing these small features present in the computer aided design (CAD) model before attempting to produce a mesh suitable for finite element analysis.

CAD and numerical simulations are still far from being integrated in a seamless manner. NURBS-enhanced finite element method (NEFEM) was proposed to bridge this gap between [15] by defining curved elements in contact with the CAD boundary in terms of the exact boundary description. The advantages of NEFEM have been studied in detail in [16, 14] and the extension of NEFEM to three dimensional domains was presented in [17], see also the review in [18]. Despite all these benefits, the lack of an automatic mesh generator has hampered the widespread application of NEFEM. In fact, this lack of such an automatic mesh generator for NEFEM has motivated the development of methods that do not require the generation of fitted NEFEM meshes but still use the NEFEM rationale, see for instance [19, 20, 21].

A novel mesh generation technique that allows to produce triangular meshes where the elements account for the exact boundary representation of the domain irrespectively of the desired element size and the geometrical complexity is presented. The produced meshes allow to extend the NEFEM formalism introduced in [15], where it was assumed that an edge of an element must be defined by at most one curve. A technique to extend the meshes to higher order by using a solid mechanics analogy is also proposed. Several examples demonstrate the applicability and potential of the proposed mesh generation technique.

2 NURBS-enhanced FEM fundamentals

An two dimensional domain Ω is considered, whose boundary is represented by non-uniform B-spline (NURBS) [22] curves $\boldsymbol{C}^k$ for $k = 1, \ldots, M$, with M the total number of boundary curves and a regular partition of the domain $\overline{\Omega} = \bigcup_e \overline{\Omega}_e$ in triangles is assumed.

An element edge Γ in contact with the NURBS boundary is defined by

$$\Gamma := \bigcup_{j=1}^{N_C} \boldsymbol{C}_j([\lambda_1^j, \lambda_2^j]) \tag{1}$$

where $\boldsymbol{x}_1$ and $\boldsymbol{x}_2$ are the edge vertices, N_C the total number of curves defining the edge Γ, $\boldsymbol{C}_1(\lambda_1^1) = \boldsymbol{x}_1$ and $\boldsymbol{C}_{N_C}(\lambda_2^{N_C}) = \boldsymbol{x}_2$.

Assuming that the boundary of the element $\partial\Omega_e$ is a closed piecewise curve formed by trimmed NURBS curves and straight segments, the element Ω_e can be defined as

$$\Omega_e := \{\boldsymbol{x} \in \Omega \ \mid \ \mathrm{ind}_{\partial\Omega_e}(\boldsymbol{x}) \text{ is odd}\}$$

where $\mathrm{ind}_{\partial\Omega_e}$ is the index number of a point $\boldsymbol{x}$ with respect to the closed curve $\partial\Omega_e$.

Two properties characterise NEFEM compared to a classical isoparametric finite element formulation [14]. Firstly, the polynomial approximation is defined in the physical space, rather than in the reference element. Secondly, NEFEM uses the exact boundary representation of the domain to compute the integrals appearing in a weak variational formulation. For instance, a boundary integral along an edge on the boundary given by (1) is computed as

$$\int_\Gamma f(x,y)\, d\ell = \sum_{j=1}^{N_C} \int_{\lambda_1^j}^{\lambda_2^j} f\big(\boldsymbol{C}_j(\lambda)\big)\, \|\boldsymbol{C}_j'(\lambda)\|\, d\lambda$$

for a generic function f, see [23] for further details.

3 Generation of NEFEM meshes

3.1 Boundary discretisation

A set of sampling points is first defined on each NURBS curve on the boundary by utilising the distribution function described in [24]. The distribution of sampling point is then refined in regions where the distance from the straight sided segment connecting two sampling points and the true CAD boundary is more than a specified tolerance. Using the spacing distribution function, the desired mesh spacing at the sampling points is computed. Finally, when the spacing induces smaller elements that a specified tolerance, the spacing of the sampling points is checked and corrected.

Once the sampling points are generated, boundary curves are combined into *loops*. A loop is a collection of boundary curves $\boldsymbol{L} := \{\boldsymbol{C}_k\}_{k=1,\dots,N_L}$, where N_L is the total number of curves forming the loop, $\boldsymbol{C}_1(0) = \boldsymbol{C}_{N_L}(1)$ and $\boldsymbol{C}_k(1) = \boldsymbol{C}_{k+1}(0)$ for $k = 1, \dots, N_L - 1$.

The curves within a loop are ordered such that the first curve, $\boldsymbol{C}_1$, is of minimum length, where the length of a curve $\boldsymbol{C}_k$ trimmed to the subspace of the parametric space $[\lambda_i, \lambda_j]$ is

$$L_k([\lambda_i,\lambda_j]) := \int_{\boldsymbol{C}_k([\lambda_i,\lambda_j])} d\ell = \int_{\lambda_i}^{\lambda_j} \|\boldsymbol{C}_k'(\lambda)\|\, d\lambda$$

and the total length of the loop is by $L = \sum_{k=1}^{N_L} L_k([0,1])$.

For a given vertex $\boldsymbol{x}_{i-1}$, a candidate boundary vertex $\boldsymbol{x}_i$ at a distance $h(\boldsymbol{x}_{i-1})$ is first identified. As the objective is to enable the creation of edges across different curves, it is necessary to find the curve where the candidate vertex belongs, $\boldsymbol{C}_s$, and the associated parametric coordinate, λ_i.

In the next step, the mesh front formed by $\boldsymbol{x}_{i-1}$ and the candidate $\boldsymbol{x}_i = \boldsymbol{C}_s(\lambda_i)$ is checked, to guarantee that a valid element exists and can be built in the next stage of the proposed meshing technique. For a given edge Γ, the *horizon* of a vertex $\boldsymbol{x}_k$ of Γ is defined as the most distant point $\boldsymbol{x}_k^\star \in \Gamma$ that can be connected to $\boldsymbol{x}_k$ without intersecting Γ, as shown in Figure 1.

If the distance from the intersection of the lines connecting the boundary vertices and their corresponding horizons, $\boldsymbol{P}$, to the boundary vertices is less than the desired spacing, an interior node to form a triangle with the required spacing can be found. In this case, the second boundary vertex $\boldsymbol{x}_i$ is accepted and, otherwise, the second candidate is defined as the most distant sampling points that generates a valid front.

3.2 Domain discretisation

Given two vertices of a valid front, $\boldsymbol{x}_1^\star$ and $\boldsymbol{x}_2^\star$, and the intersection of the lines connecting the vertices and their horizons, a line of search is defined as the angle bisector of the two lines

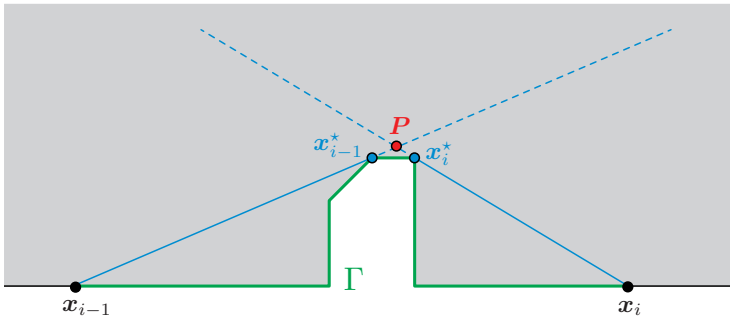

Figure 1: Illustration of the procedure to check the validity of a mesh front.

connecting the boundary vertices and their respective horizons, illustrated by a dashed red line in Figure 2. The third vertex of the element is defined as

$$\boldsymbol{x}_3 := \boldsymbol{P} + t\boldsymbol{n}_{\boldsymbol{P}} \tag{2}$$

where t takes the maximum value that guarantees that the edges $\overline{\boldsymbol{x}_1\boldsymbol{x}_3}$ and $\overline{\boldsymbol{x}_2\boldsymbol{x}_3}$ do not intersect the boundary and have length not greater than the desired element size h.

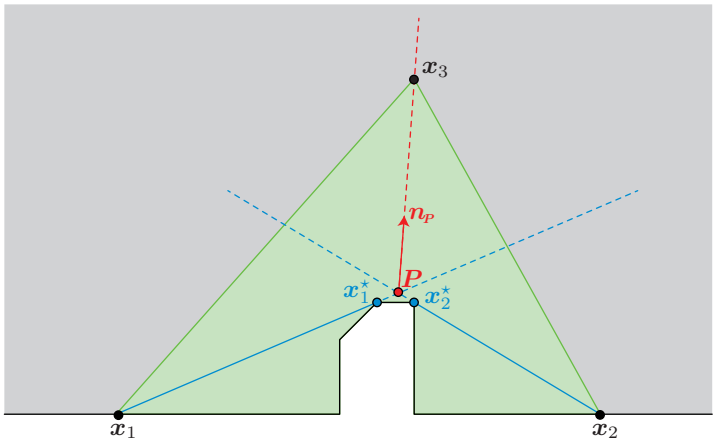

Figure 2: Illustration of the technique to build a triangular element.

3.3 Numerical integration cells

To perform the numerical integration on a NEFEM element, a recursive approach to subdivide an element in integration cells with, at most, one edge defined by a NURBS curve is devised. The integrations cells with an edge on the boundary are defined as a convex linear combination of the curved edge and the interior node as

$$\boldsymbol{\psi}_{\boldsymbol{x}_3}(\lambda, \vartheta) := (1 - \vartheta)\boldsymbol{C}(\lambda) + \vartheta\boldsymbol{x}_3 \tag{3}$$

where $\boldsymbol{x}_3$ denotes the internal vertex and $\boldsymbol{C}$ is the curve defining the boundary. This enables to build a composite two dimensional quadrature for elements in contact with the NURBS boundary.

The proposed algorithm uses a point interior to the domain, $\boldsymbol{Q}$ to check the visibility of the sampling points. The point $\boldsymbol{Q}$ is selected to be the interior node if the element has only one edge defined by NURBS as illustrated in the example of Figure 3. Otherwise, the point $\boldsymbol{Q}$ is selected to be the mid point of the only internal edge.

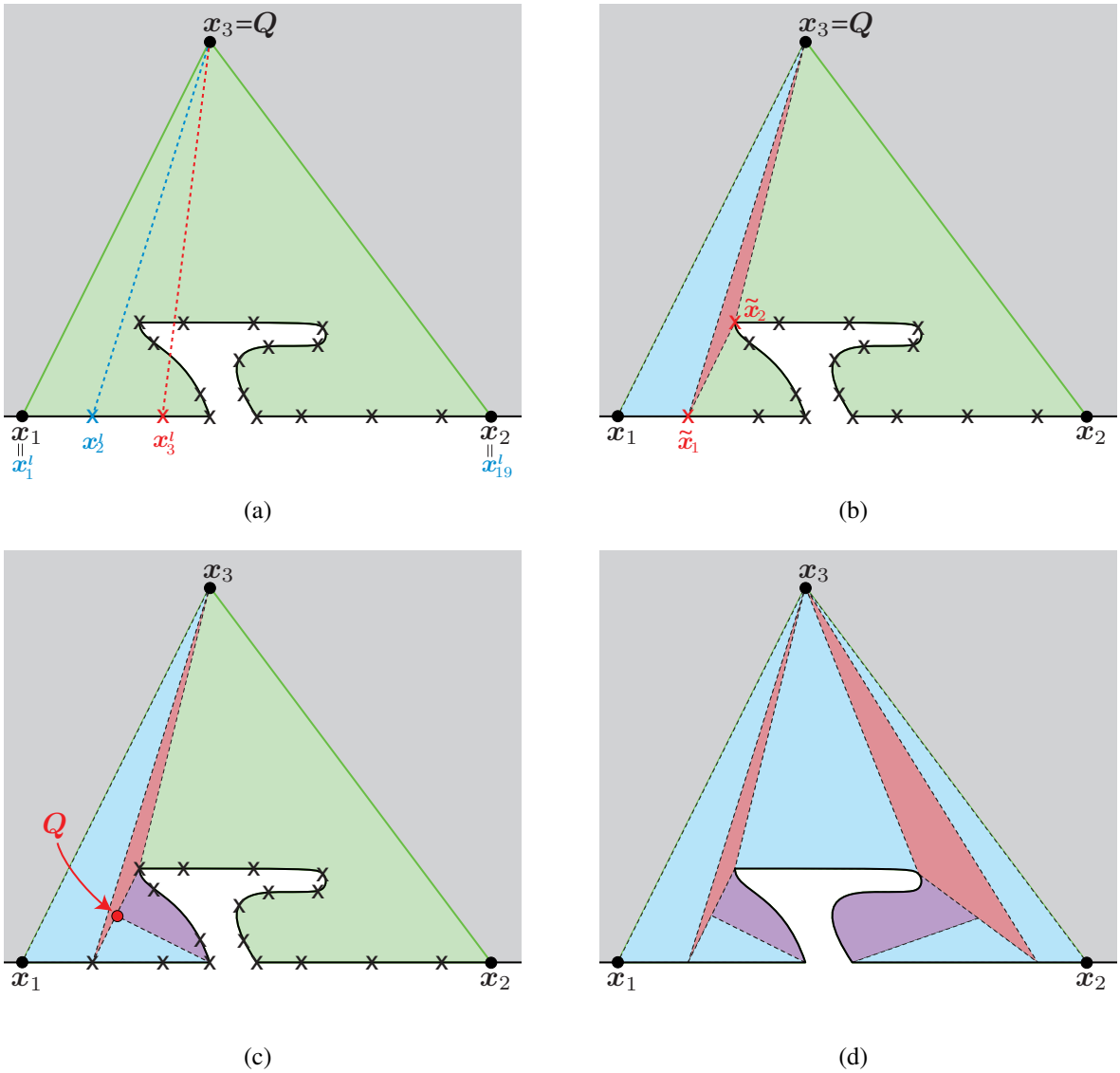

Figure 3: Illustration of the procedure to build the integration cells of an element. (a) Checking the visibility of sampling points, (b) formation of the the first two cells, (c) recursive application of the algorithm and (d) final partition of integration cells.

The visibility of each sampling points is checked until a non-visible point is found, the third sampling point in the example of Figure 3(a). Using the last visible point, two integration cells are built (red and blue cells in Figure 3(b)). The definition of the interior $\boldsymbol{Q}$ is then changed and the algorithm is applied to the triangle formed by $\tilde{\boldsymbol{x}}_1$, $\tilde{\boldsymbol{x}}_2$ and $\boldsymbol{Q}$, producing two new cells as illustrated in Figure 3(c). The procedure continues until the element is completely partitioned in integration cells as shown in Figure 3(d).

3.4 Extension to higher order elements

The strategy to extend the produced mesh to high-order is based on a linear elastic analogy [10] but the solution of the solid mechanics problem is performed element by element to ensure that the interior edges are kept as straight segments.

For an element Ω_e with at least one edge on the NURBS boundary, the triangle formed by its vertices is denoted by T_e. A high-order nodal distribution of the desired degree p is placed in T_e and a linear elastic problem is solved, assuming that the domain is an elastic medium and the Dirichlet boundary conditions are the displacements required to place the high-order edge nodes over the true (CAD) boundary. After solving the elastic problem, a high-order nodal distribution is obtained in the element Ω_e containing the exact description of the geometry.

4 Examples

4.1 Low-order mesh of a plate with a thin rectangular inclusion

The first example involves the generation of a NEFEM mesh of a square plate with a thin rectangular inclusion. The geometry of the inclusion is described using four NURBS curves (straight segments in this case) and the outer boundary is treated in the usual hierarchical manner. The total number of elements and nodes is 1,353 and 732 respectively, with only 11 elements with an edge on the NURBS boundary. It can be observed that the element size of the produced mesh is almost uniform, despite the discrepancy between the desired element size and the thickness of the inclusion.

A close view of the mesh around the inclusion is depicted in Figure 4, where it can be clearly observed that the element size is completely independent on the thickness of the inclusion. Two elements in contact with the boundary have one edge defined by two different NURBS curves. The integration cells, obtained by following the strategy presented in Section 3.3, are also shown in Figure 4.

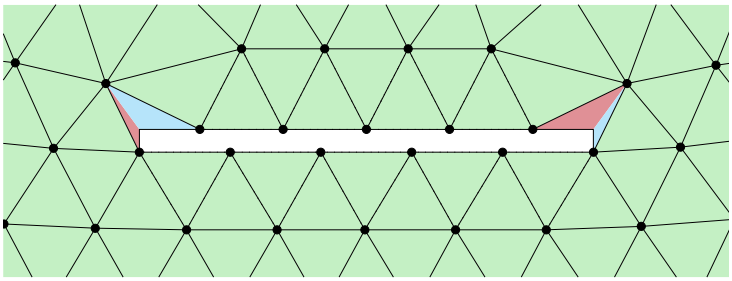

Figure 4: Detail of the NEFEM mesh near the inclusion

The minimum and maximum element edge length on the boundary is approximately 1.8 and 2.0 respectively, illustrating the ability of the proposed approach to discretise the boundary with a desired element size, irrespectively of small geometric features.

In this example, the main advantage of the proposed meshing technique is not to reduce the number of elements compared to a traditional FE mesh but to avoid the small elements introduced by a standard FE mesh generator to capture the thickness of the inclusion.

4.2 High-order mesh around an aircraft profile

The second example involves the generation of a NEFEM mesh around the aircraft profile represented in Figure 5. The detailed view of the front part shows a number of very small features compared to the size of the aircraft.

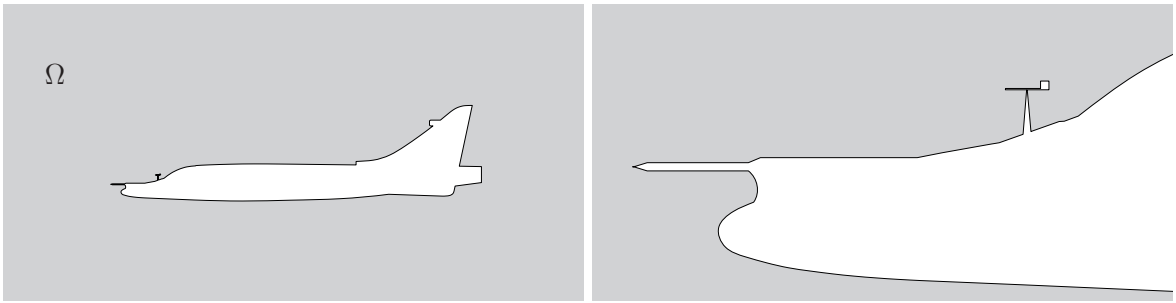

(a) (b)

Figure 5: (a) Domain Ω representing the exterior of an aircraft profile and (b) detailed view of the domain showing a number of small geometric features.

The aircraft profile is described by 53 NURBS curves, where the length of these curves differ in more than six orders of magnitude. A NEFEM mesh with uniform desired element size 2000 times larger than the shortest curve is shown in Figure 6. Two detailed view of the mesh near

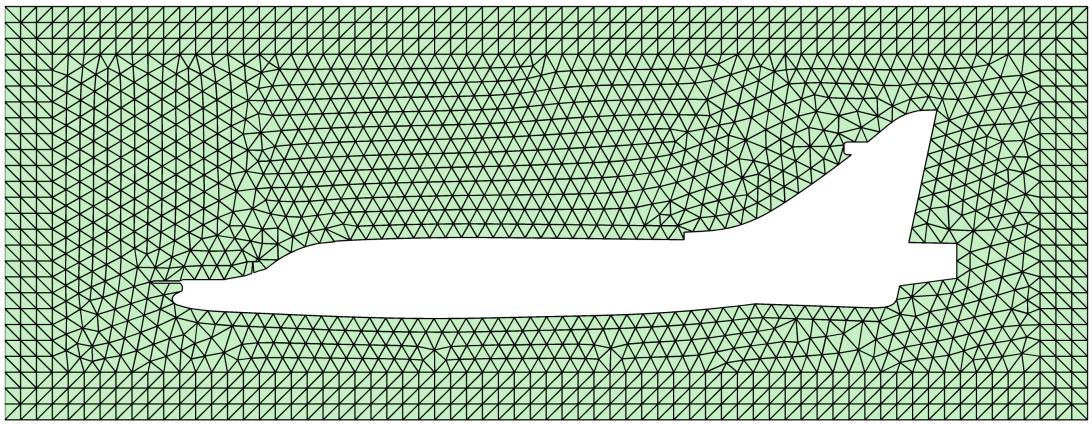

Figure 6: NEFEM mesh around a complex aircraft profile.

the most critical zones are shown in Figure 7, illustrating the integration cells used in some elements that contain edges formed by several NURBS curves.

The minimum and maximum length of the edges on the NURBS boundary generated using the proposed approach are 0.03 and 0.05 respectively, illustrating the ability to maintain the desired element size independently on the complexity of the NURBS boundary representation of the domain.

Next, the mesh is extended to high-order using the proposed solid mechanics analogy only for elements with one or more edges on the boundary. The generated mesh for a degree of approximation p=5 is shown in Figure 8.

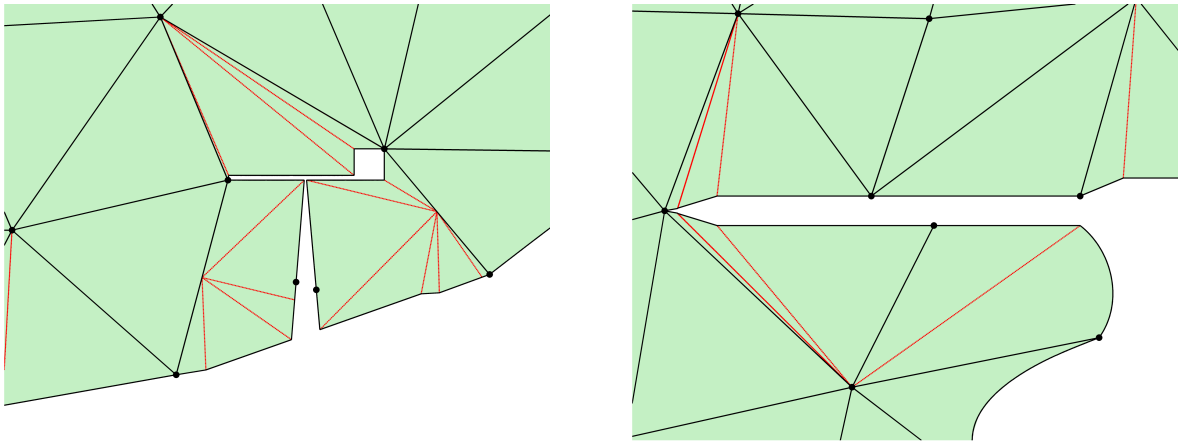

(a) (b)

Figure 7: Details of the NEFEM mesh of Figure 6 near the regions containing the two shortest NURBS curves. The black dots denote the element vertices and the red lines are the integration cells.

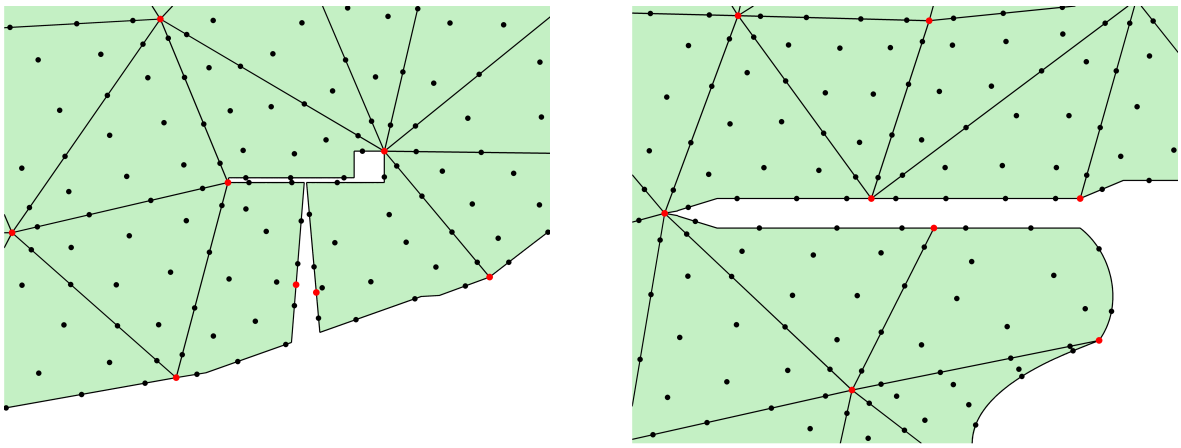

(a) (b)

Figure 8: Detail of the NEFEM mesh and the high-order nodal distribution adapted to the exact geometry. Red dots denote the element vertices.

5 Concluding remarks

A technique to produce meshes that account for the CAD boundary representation of the domain given by NURBS curves and with an element size independent on the geometric complexity of the computational domain has been presented. A methodology to extend the generated meshes to an arbitrary order is proposed and several examples demonstrate the applicability and potential of the proposed mesh generation technique.

REFERENCES

[1] J. S. Hesthaven and T. Warburton, "Nodal high-order methods on unstructured grids I. time-domain solution of Maxwell's equations," *Journal of Computational Physics*, vol. 181, no. 1, pp. 186–221, 2002.

[2] M. Ainsworth, "Dispersive and dissipative behaviour of high order discontinuous Galerkin finite element methods," *Journal of Computational Physics*, vol. 198, no. 1, pp. 106–130, 2004.

[3] R. Sevilla, O. Hassan, and K. Morgan, "The use of hybrid meshes to improve the efficiency of a discontinuous Galerkin method for the solution of Maxwells equations," *Computers & Structures*, vol. 137, pp. 2–13, 2014.

[4] H. Luo, J. D. Baum, and R. Löhner, "A fast, p-multigrid Discontinuous Galerkin method forcompressible flows at all speeds," in *Proceedings of the 44th AIAA Aerospace Sciences Meeting and Exhibit*, (Reno, Nevada), AIAA, January 2006.

[5] R. Sevilla, O. Hassan, and K. Morgan, "An analysis of the performance of a high-order stabilised finite element method for simulating compressible flows," *Computer Methods in Applied Mechanics and Engineering*, vol. 253, pp. 15–27, 2013.

[6] Z. Wang, K. Fidkowski, R. Abgrall, F. Bassi, D. Caraeni, A. Cary, H. Deconinck, R. Hartmann, K. Hillewaert, H. Huynh, *et al.*, "High-order CFD methods: current status and perspective," *International Journal for Numerical Methods in Fluids*, vol. 72, no. 8, pp. 811–845, 2013.

[7] H. Huynh, Z. J. Wang, and P. Vincent, "High-order methods for computational fluid dynamics: a brief review of compact differential formulations on unstructured grids," *Computers & Fluids*, vol. 98, pp. 209–220, 2014.

[8] M. S. Shephard, J. E. Flaherty, K. E. Jansen, X. Li, X. Luo, N. Chevaugeon, J.-F. Remacle, M. W. Beall, and R. M. O'Bara, "Adaptive mesh generation for curved domains," *Applied Numerical Mathematics*, vol. 52, no. 2-3, pp. 251 – 271, 2005.

[9] P.-O. Persson and J. Peraire, "Curved mesh generation and mesh refinement using lagrangian solid mechanics," in *Proceedings of the 47th AIAA Aerospace Sciences Meeting and Exhibit*, AIAA, 2009.

[10] Z. Q. Xie, R. Sevilla, O. Hassan, and K. Morgan, "The generation of arbitrary order curved meshes for 3D finite element analysis," *Computational Mechanics*, vol. 51, no. 3, pp. 361–374, 2013.

[11] T. Toulorge, C. Geuzaine, J.-F. Remacle, and J. Lambrechts, "Robust untangling of curvilinear meshes," *Journal of Computational Physics*, vol. 254, pp. 8–26, 2013.

[12] A. Gargallo-Peiró, X. Roca, J. Peraire, and J. Sarrate, "Distortion and quality measures for validating and generating high-order tetrahedral meshes," *Engineering with Computers*, vol. 31, no. 3, pp. 1–15, 2014.

[13] D. Moxey, D. Ekelschot, U. Keskin, S. Sherwin, and J. Peiró, "A thermo-elastic analogy for high-order curvilinear meshing with control of mesh validity and quality," *Procedia Engineering*, vol. 82, no. 0, pp. 127 – 135, 2014. 23rd International Meshing Roundtable (IMR23).

[14] R. Sevilla, S. Fernández-Méndez, and A. Huerta, "Comparison of high-order curved finite elements," *International Journal for Numerical Methods in Engineering*, vol. 87, no. 8, pp. 719–734, 2011.

[15] R. Sevilla, S. Fernández-Méndez, and A. Huerta, "NURBS-enhanced finite element method (NEFEM)," *International Journal for Numerical Methods in Engineering*, vol. 76, no. 1, pp. 56–83, 2008.

[16] R. Sevilla, S. Fernández-Méndez, and A. Huerta, "NURBS-enhanced finite element method for Euler equations," *International Journal for Numerical Methods in Fluids*, vol. 57, no. 9, pp. 1051–1069, 2008.

[17] R. Sevilla, S. Fernández-Méndez, and A. Huerta, "3D-NURBS-enhanced finite element method (NEFEM)," *International Journal for Numerical Methods in Engineering*, vol. 88, no. 2, pp. 103–125, 2011.

[18] R. Sevilla, S. Fernández-Méndez, and A. Huerta, "NURBS-enhanced finite element method (NEFEM): A seamless bridge between CAD and FEM," *Archives of Computational Methods in Engineering*, vol. 18, no. 4, pp. 441–484, 2011.

[19] G. Legrain, "A NURBS enhanced extended finite element approach for unfitted CAD analysis," *Computational Mechanics*, vol. 52, no. 4, pp. 913–929, 2013.

[20] R. Sevilla and E. Barbieri, "NURBS distance fields for extremely curved cracks," *Computational Mechanics*, vol. 54, no. 6, pp. 1431–1446, 2014.

[21] O. Marco, R. Sevilla, Y. Zhang, J. J. Ródenas, and M. Tur, "Exact 3D boundary representation in finite element analysis based on Cartesian grids independent of the geometry," *International Journal for Numerical Methods in Engineering*, vol. 103, no. 6, pp. 445–468, 2015.

[22] L. Piegl and W. Tiller, *The NURBS Book*. London: Springer-Verlag, 1995.

[23] R. Sevilla and S. Fernández-Méndez, "Numerical integration over 2D NURBS shaped domains with applications to NURBS-enhanced FEM," *Finite Elements in Analysis and Design*, vol. 47, no. 10, pp. 1209–1220, 2011.

[24] J. Peiró, "Surface grid generation," in *Handbook of grid generation* (J. F. Thompson, B. K. Soni, and N. P. Weatherill, eds.), ch. 19, CRC Press, 1999.